ARTICLE

Surface Energy Modification by Spin-Cast, Large-Area Graphene Film for Block Copolymer Lithography

Bong Hoon Kim,[†,§] Ju Young Kim,[†,§] Seong-Jun Jeong,[†,§] Jin Ok Hwang,[†] Duck Hyun Lee,[†] Dong Ok Shin,[†] Sung-Yool Choi,[‡] and Sang Ouk Kim[†,*]

[†]Department of Materials Science and Engineering, KI for the Nanocentury, KAIST, Daejeon 305-701, Republic of Korea, and [‡]Convergence Components and Materials Laboratory, Electronics and Telecommunication Research Institute (ETRI), Daejeon 305-701, Republic of Korea. [§]These authors contributed equally to this work.

ABSTRACT We demonstrate a surface energy modification method exploiting graphene film. Spin-cast, atomic layer thick, large-area reduced graphene film successfully played the role of surface energy modifier for arbitrary surfaces. The degree of reduction enabled the tuning of the surface energy. Sufficiently reduced graphene served as a neutral surface modifier to induce surface perpendicular lamellae or cylinders in a block copolymer nanotemplate. Our approach integrating large-area graphene film preparation with block copolymer lithography is potentially advantageous in creating semiconducting graphene nanoribbons and nanoporous graphene.

KEYWORDS: block copolymer · self-assembly · graphene · nanolithography · surface energy modification

Graphene is a monolayer of carbon atoms tightly packed into a two-dimensional honeycomb lattice. Since its unexpected isolation from natural graphite, the extraordinary properties of graphene have immediately fascinated the scientific community. The typical properties of graphene include the quantum Hall effect at room temperature,[1,2] the ambipolar electric field effect,[3] a tunable band gap,[4] and high elasticity,[5] which hold great promise for many technological fields such as nanoelectronics,[6,7] sensors,[8] composites,[9] and energy conversion/storage.[10,11] While a considerable body of research has been devoted to investigating these novel properties, the surface energy of graphene has rarely been investigated yet. Given that graphene is one of the thinnest materials ever known, it can serve as a highly effective surface energy modifier.

Modification of surface energy affords precise control over the surface and interfacial properties, ranging from wetting to adhesion, of a material. In the particular case of block copolymer thin films, surface modification is crucial for controlling the orientation of nanoscale domains, which is required to fully exploit the potential of these materials for nanolithographic templates. On a chemically neutral surface, the surface energy to each block of a given copolymer is balanced such that surface perpendicular nanoscale cylinders or lamellae are assembled within a thin film confinement.[12−15] The block copolymer thin films with such surface perpendicular nanodomains are attractive self-assembled nanotemplates. The vertical side wall profiles of such morphologies ensure facile and robust pattern transfer by further etching or deposition.[12−15]

Herein, we introduce a straightforward surface energy modification method using large-area reduced graphene film. Our approach relies on the thermal or chemical reduction of spin-cast graphene oxide film to tune the surface energy. To date, various synthesis methods for graphene, such as mechanical exfoliation,[3] thermal decomposition of SiC,[16] reduction of graphene oxide,[17] liquid-phase exfoliation of graphite,[18] and chemical vapor deposition (CVD),[19] have been exploited. Among them, the chemical oxidation of natural graphite and the subsequent reduction is a truly scalable method for wrinkle-free, large-area graphene film. In our approach, neutral surface modification with spin-cast reduced graphene films successfully induced the surface perpendicular lamellae or cylinders in block copolymer thin films, which play a role as a lithographic mask for further nanofabrication. This strategy exhibits a number of advantages: (i) a rapid and straightforward processing, intrinsically scalable to arbitrary large-area processing, is established; (ii) noncovalent surface modification universally applicable to various substrates, including inert substrates such as Au or polymers, and nonplanar substrates, and flexible/stretchable substrates, is possible;

*Address correspondence to sangouk.kim@kaist.ac.kr.

Received for review July 1, 2010 and accepted August 16, 2010.

Published online August 25, 2010. 10.1021/nn101491g

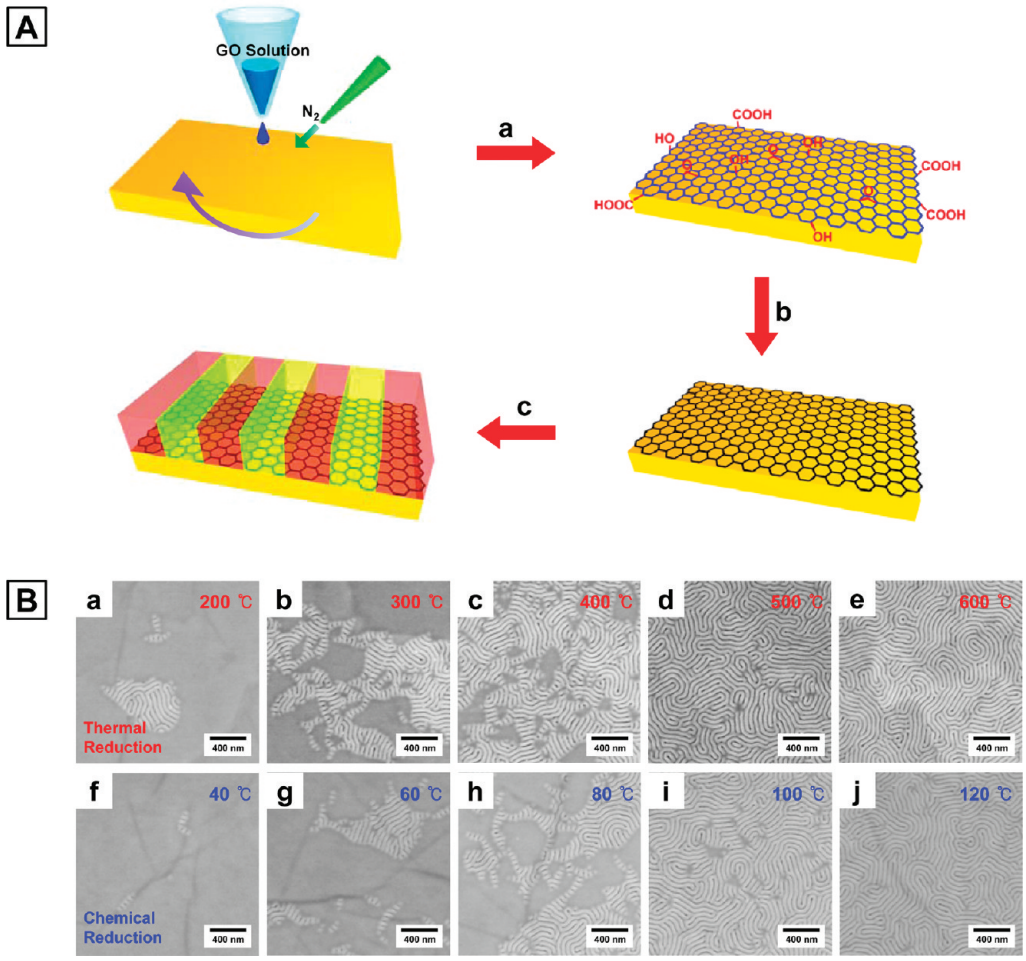

Figure 1. (A) Schematic representation of graphene film surface modification. (a) Spin-casting of graphene oxide thin film on various substrates assisted by N_2 gas blowing. (b) Thermal or chemical reduction. (c) Spin-casting a PS-*b*-PMMA thin film and thermal annealing for self-assembly. (B) SEM images of PS-*b*-PMMA thin films self-assembled upon graphene films thermally or chemically reduced at various temperatures. The reduction was performed thermally at (a) 200 °C, (b) 300 °C, (c) 400 °C, (d) 500 °C, and (e) 600 °C or chemically at (f) 40 °C, (g) 60 °C, (h) 80 °C, (i) 100 °C, and (j) 120 °C.

(iii) a highly flat, electroconductive, mechanically flexible surface modification layer is ensured; and (iv) conventional lithographic approaches are compatible for generating surface energy modulated substrates.

RESULTS AND DISCUSSION

The overall process of our surface modification using large-area reduced graphene film is schematically described in Figure 1A. Various substrate materials including metals, semiconductors, ceramics, or polymers were prepared by thin film deposition methods.[14] The substrate surfaces were cleaned by UVO irradiation before graphene film deposition. Graphene oxide was produced by oxidizing natural graphite using a modified Hummers method.[17,20,21] Fully exfoliated graphene oxides sheets were separated by centrifuge and resuspended in the mixed solvent of water and methanol. A graphene oxide thin film was deposited from this fully exfoliated solution onto various substrates by a spin-casting assisted by nitrogen gas blowing (Figure 1A.a).[22] We note that, unlike CVD or other graphene film preparation methods, spin-casting enabled wrinkle-free, highly uniform graphene film preparation over a large area. This wrinkle-free morphology is crucial for the subsequent large-area block copolymer nanotemplate preparation and pattern transfer. After deposition, the graphene oxide thin film was thermally or chemically reduced (Figure 1A.b).[17,23] A lamellar or cylindrical polystyrene-*block*-poly(methyl methacrylate) (PS-*b*-PMMA) thin film (80 nm) was spin-cast on the reduced graphene film and thermally annealed at a high temperature (200−280 °C) to generate a surface perpendicular lamellar or hexagonal cylinder nanotemplate (Figure 1A.c).

Figure 1B presents plane view SEM images of lamellar block copolymer thin film morphologies on graphene films at various reduction temperatures (a−e, thermal reduction under hydrogen atmosphere; f−j, chemical reduction with hydrazine monohydrate vapor). A number of processing parameters, such as the hydrogen gas flow rate in thermal reduction or hydrazine monohydrate vapor pressure in chemical reduction, may influence the reduction of graphene film. Among them, the most critical parameter was found

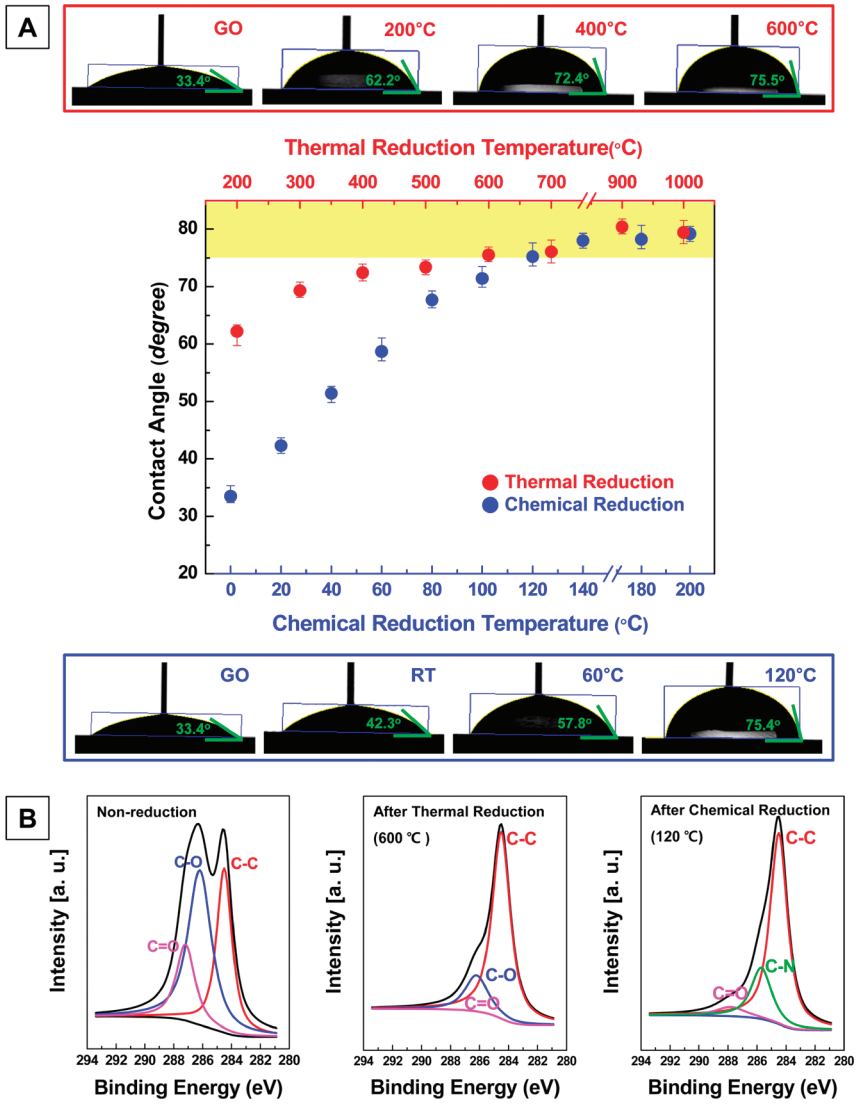

Figure 2. (A) Advancing water contact angles measured upon reduced graphene films prepared at various reduction temperatures. The advancing water contact angle entered the neutral window for PS-*b*-PMMA block copolymer (contact angle = 75−85°) at 600 °C for thermal reduction and 120 °C for chemical reduction. Surface perpendicular lamellar or cylinder morphology was self-assembled upon the neutral graphene film. (B) XPS C1s peaks of graphene oxide and reduced graphene after thermal (600 °C) and chemical reduction (120 °C).

to be the reduction temperature for both thermal and chemical reduction. As shown in Figure 1B, surface perpendicular nanodomains were achieved over the entire block copolymer film above 600 °C for thermal treatment and 120 °C for chemical treatments. Below the critical temperatures, the underlying graphene oxide film was insufficiently reduced with a significant amount of polar oxygen functional groups remaining at the basal plane and edge. As a result, the polar PMMA block preferentially segregates at the block copolymer film/graphene oxide film interface, inducing surface parallel lamellar morphology. In contrast, above the critical temperatures, the underlying graphene film was sufficiently reduced to become neutral to PS-*b*-PMMA block copolymers (the same interfacial tension for PS and PMMA blocks). In this condition, lamellar or cylinder nanodomains spontaneously orient in the surface perpendicular direction due to the confinement from the thin film geometry. Several seconds or minutes of reduction were sufficient to induce surface perpendicular nanodomains.

Figure 2A shows the variation of the water contact angle on the reduced graphene film as a function of reduction temperature. It has been reported that organic modified substrates with a water contact angle of 75−85° may induce surface perpendicular lamellar or cylinder nanodomains of PS-*b*-PMMA.[13] The advancing water contact angle on reduced graphene film entered this neutral window when the thermal reduction temperature and chemical reduction temperature were 600 and 120 °C, respectively. These results are quantitatively consistent with the experimental observation of nanodomain orientation presented in Figure 1B. We note that the water contact angle of reduced graphene film saturated around 80° upon a further increase of the reduction temperature over the critical temperatures. The interfacial tensions of PS and PMMA homopolymers to reduced graphene film were also straightforwardly measured by contact angle measurements of molten PS and PMMA droplets upon reduced graphene film (Supporting Information). The similar values of 26.31 and 26.37 mJ/m^2 were obtained for PMMA and PS components, respectively, confirming the neutrality of reduced graphene film.

The basal plane and edge of graphene oxide are known to be decorated with polar oxygen containing functional groups such as epoxide, hydroxyl, carbonyl, and carboxyl groups.[24−31] The evolution of the surface chemistry of graphene oxide film before and after thermal or chemical reduction was monitored by X-ray photoelectron spectroscopy (XPS) (Figure 2B).[23] Before reduction, the C1s peak of the graphene oxide consisted of a sp^2 carbon peak (C−C, 284.5 eV) and higher binding energy sp^3 carbon peaks such as C−O (286.2 eV) and C═O (carbonyls, 287.8 eV) peaks. The relative intensities of those C−O and C═O peaks dramatically decreased after thermal or chemical reduction. This confirmed the decrease of polar oxygen functional groups upon thermal or chemical reduction. Such a decrease of the polar oxygen functional groups rendered the graphene surface less polar and, eventually, the reduced graphene sur-

face became neutral to PS-*b*-PMMA and induced surface perpendicular lamellar or cylinder nanodomains. We note that a negligible intensity of polar C−N peak (285.7 eV) was observed after chemical reduction. This was attributed to the partial transformation of carbonyl functionalities into hydrazine groups.[23]

Facile deposition of large-area reduced graphene film upon arbitrary substrates *via* spin-casting and reduction enables an unprecedented surface energy modification method generally applicable to arbitrary substrates including chemically inert surfaces such as gold or polymers.[14] Figure 3 shows scanning electron microscopy (SEM) images of block copolymer thin films with surface perpendicular lamellar or cylinder nanodomains prepared on metal (gold, Figure 3A), semiconductors (silicon, Figure 3E,F), ceramics (silicon oxide and titania, Figure 3B,C), and polymer (polyimide, Figure 3D) substrates. Reduced graphene films were deposited on all substrates and mediated the neutral surface energy for surface perpendicular lamellar or cylinder nanodomains. When the annealing temperature was high enough (250 °C) to have a neutral interface with vacuum,[32] the cylinder or lamellar nanodomains in a PS-*b*-PMMA thin film vertically oriented throughout the film thickness over 200 nm. We used the same approach for other substrates, such as Ru, Ti, Pt, and SiN, and succeeded in preparing block copolymer thin films with surface perpendicular nanodomains. It is noteworthy that, despite the atomic scale thickness of graphene flakes, the layer number of spin-cast graphene film does not significantly influence the surface energy. Surface perpendicular nanodomains could be prepared on either single-layer (Figure 3E, Supporting Information Figure S1) or thick multilayer graphene (about 10 layers) (Figure 3F). Figure 3E presents a plane view SEM image of lamellar PS-*b*-PMMA block copolymer film self-assembled on a single-layer reduced graphene flakes. The inset shows the shape of the graphene flake remaining on the silicon substrate after removing block copolymer film. The shape exactly matches the surface perpendicular lamellar morphology region. Upon the surrounding bare silicon substrate region, block copolymer lamellae were oriented in the surface-parallel direction, revealing featureless in-plane morphology. Figure 3F shows surface perpendicular lamellar morphology assembled on a multilayer crumpled graphene film. Owing to the mechanical flexibility of graphene film, surface perpendicular lamellae were assembled on such nonplanar geometry. Since flexible graphene film can be readily transferred to nonplanar substrates or flexible/stretchable substrates *via* wet or dry transfer methods, the graphene neutral layer is useful for potential use of block copolymer lithography in the nanopatterning of nonplanar three-dimensional geometry surfaces or flexible/stretchable nanodevice structures.[21,33−36] We note that our approach of using graphene film as block copolymer lithography substrate is also useful for other widely used block copolymers, such as polystyrene-*block*-poly(ethylene oxides) (PS-*b*-PEOs), polystyrene-*block*-poly(2-vinylpyridine) (PS-*b*-P2VP), and PS-*b*-P4VP. The solvent evaporation assisted vertical nanodomain alignment of those block copolymers does not require neutral surface.[37] Nonetheless, the mechanical flexibility and transferability of graphene film are still beneficial for the nanopatterning of nonplanar or flexible substrates (Supporting Information Figure S2).

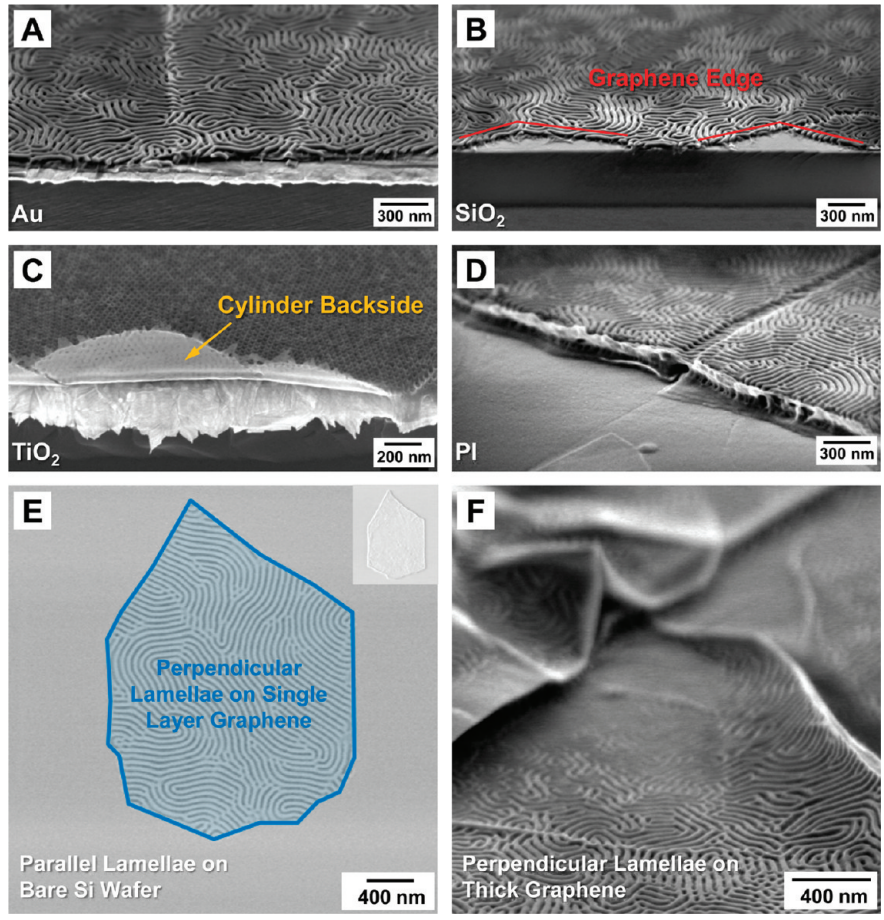

Figure 3. Tilted 45° SEM images of surface perpendicular lamellar or cylinder nanotemplates of PS-*b*-PMMA (lamellar period = 48 nm, center-to-center distance between neighboring cylinders = 42 nm) self-assembled on (A) Au, (B) SiO_2, (C) TiO_2, and (D) polyimide substrates with reduced graphene neutral layer. PS-*b*-PMMA block copolymer thin films with surface perpendicular lamellar morphologies self-assembled on either (E) single-layer graphene flake or (F) multilayer graphene film. The inset in panel E shows the graphene flake remaining after removing block copolymer film.

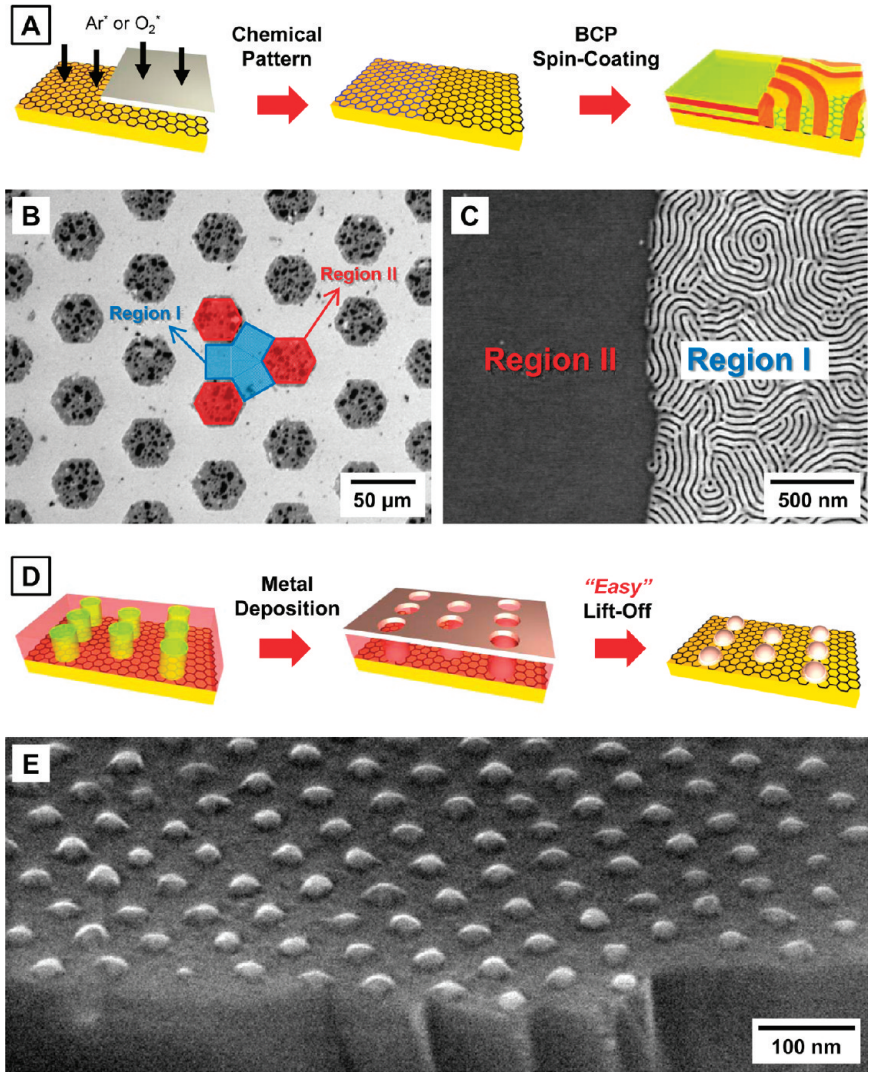

Figure 4. (A) Schematic illustration for the chemical patterning of graphene film using selective etching and the resultant lamellar block copolymer morphology. (B) Low- and (C) high-magnification SEM images of lamellar block copolymer film self-assembled on a chemically patterned graphene layer. Region I was protected against RIE by the Cu TEM grid, while Region II was etched. (D) Schematic illustration of nickel nanodot array generation. After the selective removal of PMMA domains of a PS-*b*-PMMA cylinder nanotemplate, nickel film was deposited by conventional thermal evaporation. (E) Tilted 45° view of SEM images of nickel dot arrays generated *via* block copolymer lithography assisted by neutral graphene film layer.

We have presented the versatility of graphene film to produce surface perpendicular lamellar or cylinder nanodomains in block copolymer thin films. For further utilization of block copolymer lithography in device-oriented nanofabrication, the directed assembly into laterally ordered morphology is highly demanded.[12,37−43] In order to achieve such a directed assembly, chemically prepatterned substrates have been frequently utilized. As shown in Figure 4, the graphene film neutral layer is compatible to the chemical patterning process. Figure 4A schematically depicts the chemical patterning process relying on the selective oxidation or selective etching of the graphene neutral layer by argon or oxygen RIE. The copper TEM grid with hexagonal openings was used as a shadow mask to impose the selective RIE. After RIE, a block copolymer thin film was spin-cast on the chemically patterned graphene film and self-assembled *via* high-temperature annealing. Figure 4B,C shows the SEM images of the resultant block copolymer morphologies observed at a low and high magnification. In the low-magnification image (Figure 4B), the different orientations of lamellar nanodomains provide the image contrast in the plane view. The areas exposed to RIE (Region II) exhibited featureless in-plane morphology of surface parallel lamellae, while the area protected by a TEM grid (Region I) maintained the neutral surface energy and, thus, showed surface perpendicular lamellar morphology. Figure 4C shows the sharp morphology distinction at the boundary between surface parallel and perpendicular lamellar regions. This sharp morphology distinction demonstrates the chemical patternability of the graphene layer into fine nanoscale patterns, which is greatly advantageous for the directed assembly of block copolymer into device-oriented nanostructures. We note that the chemical patterning of graphene film required a very low dose of RIE, which is attributed to its extremely thin thickness. In addition, owing to the electroconductivity of graphene film, chemical patterning with modulated electric potential is possible. This is potentially useful for the directed assembly of charged objects such as polyelectrolytes or charged nanoparticles.

The easy lift-off of block copolymer template film is another advantage of the graphene neutral layer for block copolymer lithography (Figure 4D,E). Surface perpendicular lamellae or cylinders in PS-*b*-PMMA block copolymer film can be utilized as a lithographic mask after the selective removal of PMMA domains. Figure 4D describes selective metal deposition using a PS nanoporous mask prepared from a cylindrical PS-*b*-PMMA copolymer film. After metal deposition over the entire area, the PS nanoporous mask must be lifted off. When a neutral brush layer was used, this lift-off process typically performed *via* sonication in organic solvent took at least several hours. This is due to the strong interfacial interaction caused by the interpenetration and entanglement of the polymer brush into the block copolymer thin film. In contrast, if atomically flat graphene film was used as a neutral layer, the block copolymer nanotemplate

could be readily lifted off *via* several minutes of sonication. Figure 4E shows a 45° tilted cross-sectional SEM image of large-area nickel nanodot arrays fabricated by block copolymer lithography assisted with a reduced graphene neutral layer.

CONCLUSIONS

We have first demonstrated a promising route of using spin-cast, large-area reduced graphene film as a surface energy modifier. We found that sufficiently reduced graphene film, which can be deposited upon arbitrary substrate materials over a large area, can be effectively used as a neutral layer for PS-*b*-PMMA block copolymer nanotemplates. Further development of our approach toward directed block copolymer assembly upon chemically/topographically patterned graphene is anticipated for the large-area scalable production of nanopatterned graphene such as graphene nanoribbons, nanoporous graphene, and so on.[41,42,44−46]

METHODS

Preparation of Graphene Oxide Film: Graphene oxide was prepared from natural graphite (SP1 Bay Carbon) by a modified Hummers method. Single-layer or multilayer graphene oxide thin film was spin-cast onto various substrate materials by controlling the graphene oxide composition in methanol/water suspension. For single-layer graphene oxide flake deposition, graphene oxide solution with the weight ratio of graphene oxide/methanol/water = 1:500:2500 was used. For uniform multilayer film deposition, graphene oxide solution with the weight ratio of graphene oxide/methanol/water = 1:1750:100 was used. Spin-casting was assisted by nitrogen gas blowing at the center region. Large-area multilayer graphene oxide thin film was achieved on a 4 in. wafer surface by several repeated spin-castings.

Thermal or Chemical Reduction of Graphene: We used two methods for graphene reduction: (i) thermal treatment under H_2 gas or (ii) chemical treatment with hydrazine monohydrate vapor exposure. The thermal treatment was performed at various temperatures from 200 to 1000 °C at 100 °C intervals. Chemical treatment was also performed at various temperatures from 20 to 200 °C at 20 °C intervals.

Self-Assembled PS-*b*-PMMA Nanotemplate: A PS-*b*-PMMA block copolymer thin film was spin-cast onto reduced graphene film. The block copolymer with a molecular weight of 48−46 K or 46−21 K kg mol^{-1} for PS and PMMA blocks, respectively, was spin-cast from a toluene solution. Thermal annealing was conducted at 250 °C for 3−5 h to accomplish self-assembled morphology. The PMMA domains in a block copolymer film could be selectively removed by dry O_2 plasma RIE. The resultant nanoporous PS template was applied as a lithographic mask for further pattern transfer.

Chemical Patterning of Graphene with Selective RIE: The chemical patterning of graphene was performed *via* selective oxidation or selective etching using RIE (30 W, 40 sccm) with a Cu TEM grid shadow mask.

Characterization: The nanoscale morphology was characterized using a Hitachi S-4800 SEM with a field emission source of 1 kV. The advancing water contact angle was measured with Surface Electro Optics PNX 150. XPA data were obtained using Thermo VG Scientific ESCA 2000.

Acknowledgment. This work was supported by the National Research Laboratory Program (R0A-2008-000-20057-0), the National Research Foundation of Korea (NRF) (Grant Nos. K20722000002-10B0100-00210, 2008-0062204, 2009-0093758), the Pioneer Research Center Program (2009-0093758), and the basic research program of ETRI (10ZE1160), funded by the Korean government (MEST & MKE).

Supporting Information Available: Supporting results. This material is available free of charge *via* the Internet at http://pubs.acs.org.

REFERENCES AND NOTES

1. Novoselov, K. S.; Jiang, Z.; Zhang, Y.; Morozov, S. V.; Stormer, H. L.; Zeitler, U.; Maan, J. C.; Boebinger, G. S.; Kim, P.; Geim, A. K. Room-Temperature Quantum Hall Effect in Graphene. *Science* **2007**, *315*, 1379.
2. Zhang, Y.; Tan, Y.-W.; Stormer, H. L.; Kim, P. Experimental Observation of the Quantum Hall Effect and Berry's Phase in Graphene. *Nature* **2005**, *438*, 201–204.
3. Novoselov, K. S.; Geim, A. K.; Morozov, S. V.; Jiang, D.; Zhang, Y.; Dubonos, S. V.; Grigorieva, I. V.; Firsov, A. A. Electric Field Effect in Atomically Thin Carbon Films. *Science* **2004**, *306*, 666–669.
4. Han, M. Y.; Özyilmaz, B.; Zhang, Y.; Kim, P. Energy Band-Gap Engineering of Graphene Nanoribbons. *Phys. Rev. Lett.* **2007**, *98*, 206805-1–206805-4.
5. Lee, C.; Wei, X.; Kysar, J. W.; Hone, J. Measurement of the Elastic Properties and Intrinsic Strength of Monolayer Graphene. *Science* **2008**, *321*, 385–388.
6. Wang, X.; Ouyang, Y.; Li, X.; Wang, H.; Guo, J.; Dai, H. Room-Temperature All-Semiconducting Sub-10-nm Graphene Nanoribbon Field-Effect Transistors. *Phys. Rev. Lett.* **2008**, *100*, 206803-1–206803-4.
7. Li, X.; Cai, W.; An, J.; Kim, S.; Nah, J.; Yang, D.; Piner, R.; Velamakanni, A.; Jung, I.; Tutuc, E.; *et al.* Large-Area Synthesis of High-Quality and Uniform Graphene Films on Copper Foils. *Science* **2009**, *324*, 1312–1314.
8. Schedin, F.; Geim, A. K.; Morozov, S. V.; Hill, E. W.; Blake, P.; Katsnelson, M. I.; Novoselov, K. S. Detection of Individual Gas Molecules Adsorbed on Graphene. *Nat. Mater.* **2007**, *6*, 652–655.
9. Stankovich, S.; Dickin, A.; Dommett, G. H. B.; Kohlhaas, K. M.; Zimney, E. J.; Stach, E. A.; Piner, R. D.; Ruoff, R. S. Graphene-Based Composite Materials. *Nature* **2006**, *442*, 282–286.
10. Dikin, D. A.; Stankovich, S.; Zimney, E. J.; Piner, R. D.; Dommett, G. H. B.; Evmenenko, G.; Nguyen, S. T.; Ruoff, R. S. Preparation and Characterization of Graphene Oxide Paper. *Nature* **2007**, *448*, 457–460.
11. Stoller, M. D.; Park, S.; Zhu, Y.; An, J.; Ruoff, R. S. Graphene-Based Ultracapacitors. *Nano Lett.* **2008**, *8*, 3498–3502.
12. Kim, S. O.; Solak, H. H.; Stoykovich, M. P.; Ferrier, N. J.; De Pablo, J. J.; Nealey, P. F. Epitaxial Self-Assembly of Block Copolymers on Lithographically Defined Nanopatterned Substrates. *Nature* **2003**, *424*, 411–414.
13. Mansky, P.; Liu, Y.; Huang, E.; Russell, T. P.; Hawker, C. Controlling Polymer−Surface Interactions with Random Copolymer Brushes. *Science* **1997**, *275*, 1458–1460.
14. Jeong, S.-J.; Xia, G.; Kim, B. H.; Shin, D. O.; Kwon, S.-H.; Kang, S.-W.; Kim, S. O. Universal Block Copolymer Lithography for Metals, Semiconductors, Ceramics, and Polymers. *Adv. Mater.* **2008**, *20*, 1898–1904.
15. Ryu, D. Y.; Shin, K.; Drockenmuller, E.; Hawker, C. J.; Russell, T. P. A Generalized Approach to the Modification of Solid Surfaces. *Science* **2005**, *308*, 236–239.
16. Berger, C.; Song, Z.; Li, X.; Wu, X.; Brown, N.; Naud, C.; Mayou, D.; Li, T.; Hass, J.; Marchenkov, A. N.; *et al.* Electronic Confinement and Coherence in Patterned Epitaxial Graphene. *Science* **2006**, *312*, 1191–1196.
17. Park, S.; Ruoff, R. S. Chemical Methods for the Production of Graphenes. *Nat. Nanotechnol.* **2009**, *4*, 217–224.

18. Tung, V. C.; Allen, M. J.; Yang, Y.; Kaner, R. B. High-Throughput Solution Processing of Large-Scale Graphene. *Nat. Nanotechnol.* **2009**, *4*, 25–29.
19. Kim, K. S.; Zhao, Y.; Jang, H.; Lee, S. Y.; Kim, J. M.; Kim, K. S.; Ahn, J.-H.; Kim, P.; Choi, J.-Y.; Hong, B. H. Large-Scale Pattern Growth of Graphene Films for Stretchable Transparent Electrodes. *Nature* **2009**, *457*, 706–710.
20. Han, T. H.; Lee, W. J.; Lee, D. H.; Kim, J. E.; Choi, E.-Y.; Kim, S. O. Peptide/Graphene Hybrid Assembly into Core/Shell Nanowires. *Adv. Mater.* **2010**, *22*, 2060–2064.
21. Lee, D. H.; Kim, J. E.; Han, T. H.; Hwang, J. W.; Jeon, S. W.; Choi, S.-Y.; Hong, S. H.; Lee, W. J.; Ruoff, R. S.; Kim, S. O. Versatile Carbon Hybrid Films Composed of Vertical Carbon Nanotubes Grown on Mechanically Compliant Graphene Films. *Adv. Mater.* **2010**, *22*, 1247–1252.
22. Robinson, J. T.; Zalalutdinov, M.; Baldwin, J. W.; Snow, E. S.; Wei, Z.; Sheehan, P.; Houston, B. H. Wafer-Scale Reduced Graphene Oxide Films for Nanomechanical Devices. *Nano Lett.* **2008**, *8*, 3441–3445.
23. Becerril, H. A.; Mao, J.; Liu, Z.; Stoltenberg, R. M.; Bao, Z.; Chen, Y. Evaluation of Solution-Processed Reduced Graphene Oxide Films as Transparent Conductors. *ACS Nano* **2008**, *2*, 463–470.
24. Kinoshita, K. *Carbon: Electrochemical and Physicochemical Properties*; Wiley: New York, 1988.
25. Stankovich, S.; Kikin, D. A.; Piner, R. D.; Kohlhaas, K. A.; Kleinhammes, A.; Jia, Y. Y.; Wu, Y.; Nguyen, S. T.; Ruoff, R. S. Synthesis of Graphene-Based Nanosheets *via* Chemical Reduction of Exfoliated Graphite Oxide. *Carbon* **2007**, *45*, 1558–1565.
26. Cai, W.; Piner, R. D.; Stadermann, F. J.; Park, S.; Shaibat, M. A.; Ishii, Y.; Yang, D.; Velamakanni, A.; An, S. J.; Stoller, M.; *et al.* Synthesis and Solid-State NMR Structural Characterization of 13C-Labeled Graphite Oxide. *Science* **2008**, *321*, 1815–1817.
27. Hontoria-Lucas, C.; Loperz-Peinado, A. J.; Lopez-Gonazlez, J. de D.; Rojas-Cervantes, M. L.; Martin-Aranda, R. M. Study of Oxyen-Containing Groups in a Series of Graphite Oxides: Physical and Chemical Characterization. *Carbon* **1995**, *33*, 1585–1592.
28. He, H. Y.; Klinowski, J.; Forster, M.; Lerf, A. A New Structural Model for Graphite Oxide. *Chem. Phys. Lett.* **1998**, *287*, 53–56.
29. Lerf, A.; He, H. Y.; Forster, M.; Klinowski, J. Structure of Graphite Oxide Revisited. *J. Phys. Chem. B* **1998**, *102*, 4477–4482.
30. Gao, W.; Alemany, L. B.; Ci, L. J.; Ajayan, P. M. New Insights into the Structure and Reduction of Graphite Oxide. *Nat. Chem.* **2009**, *1*, 403–408.
31. Li, X.; Wang, H.; Robinson, J. T.; Sanchez, H.; Diankov, G.; Dai, H. Simultaneous Nitrogen Doping and Reduction of Graphene Oxide. *J. Am. Chem. Soc.* **2009**, *131*, 15939–15944.
32. Mansky, P.; Russell, T. P.; Hawker, C. J.; Mays, J.; Cook, D. C.; Satija, S. K. Interfacial Segregation in Disordered Block Copolymers: Effect of Tunable Surface Potentials. *Phys. Rev. Lett.* **1997**, *79*, 237–240.
33. Unarunotai, S.; Murata, Y.; Chialvo, C. E.; Kim, H.; MacLaren, S.; Mason, N.; Petrov, I.; Rogers, J. A. Transfer of Graphene Layers Grown on SiC Wafers to Other Substrates and Their Integration into Field Effect Transistors. *Appl. Phys. Lett.* **2009**, *95*, 202101-1–202101-3.
34. Allen, M. J.; Tung, V. C.; Gomez, L.; Xu, Z.; Chen, L.-M.; Nelson, K. S.; Zhou, C.; Kaner, R. B.; Yang, Y. Soft Transfer Printing of Chemically Converted Graphene. *Adv. Mater.* **2009**, *21*, 2098–2102.
35. Li, X.; Zhu, Y.; Cai, W.; Borysiak, M.; Han, B.; Chen, D.; Piner, R. D.; Colombo, L.; Ruoff, R. S. Transfer of Large-Area Graphene Films for High-Performance Transparent Conductive Electrodes. *Nano Lett.* **2009**, *9*, 4359–4363.
36. Lee, Y.; Bae, S.; Jang, H.; Jang, S.; Zhu, S.-E.; Sim, S. H.; Song, Y. I.; Hong, B. H.; Ahn, J.-H. Wafer-Scale Synthesis and Transfer of Graphene Films. *Nano Lett.* **2010**, *10*, 490–493.
37. Park, S.; Lee, D. H.; Xu, J.; Kim, B.; Hong, S. W.; Jeong, U.; Xu, T.; Russell, T. P. Macroscopic 10-Terabit-per-Square-Inch Arrays from Block Copolymers with Lateral Order. *Science* **2009**, *20*, 1030–1033.
38. Kim, S. O.; Kim, B. H.; Meng, D.; Shin, D. O.; Koo, C. M.; Solak, H. H.; Wang, Q. Novel Complex Nanostructure from Directed Assembly of Block Copolymers on Incommensurate Surface Patterns. *Adv. Mater.* **2007**, *19*, 3271–3275.
39. Kim, B. H.; Shin, D. O.; Jeong, S.-J.; Koo, C. M.; Jeon, S. C.; Hwang, W. J.; Lee, S.; Lee, M. G.; Kim, S. O. Hierarchical Self-Assembly of Block Copolymers for Lithography-Free Nanopatterning. *Adv. Mater.* **2008**, *20*, 2303–2307.
40. Kim, B. H.; Lee, H. M.; Lee, J.-H.; Son, S.-W.; Jeong, S.-J.; Lee, S. M.; Lee, D. I.; Kwak, S. W.; Jeong, H. W.; Shin, H. J.; *et al.* Spontaneous Lamellar Alignment in Thickness-Modulated Block Copolymer Films. *Adv. Funct. Mater.* **2009**, *19*, 2584–2591.
41. Park, S. H.; Shin, D. O.; Kim, B. H.; Yoon, D. K.; Kim, K.; Lee, S. Y.; Oh, S.-H.; Choi, S.-W.; Jeon, S. C.; Kim, S. O. Block Copolymer Multiple Patterning Integrated with Conventional ArF Lithography. *Soft Matter* **2010**, *6*, 120–125.
42. Jeong, S.-J.; Kim, J. E.; Moon, H.-S.; Kim, B. H.; Kim, S. M.; Kim, J. B.; Kim, S. O. Soft Graphoepitaxy of Block Copolymer Assembly with Disposable Photoresist Confinement. *Nano Lett.* **2009**, *9*, 2300–2305.
43. Cheng, J. Y.; Mayes, A. M.; Ross, C. A. Nanostructure Engineering by Templated Self-Assembly of Block Copolymers. *Nat. Mater.* **2004**, *3*, 823–828.
44. Li, X.; Wang, X.; Zhang, L.; Lee, S.; Dai, H. Chemically Derived, Ultrasmooth Graphene Nanoribbon Semiconductors. *Science* **2008**, *319*, 1229–1232.
45. Jiao, L.; Zhang, L.; Wang, X.; Diankov, G.; Dai, H. Narrow Graphene Nanoribbons from Carbon Nanotubes. *Nature* **2009**, *458*, 877–880.
46. Bai, J.; Zhong, X.; Jiang, S.; Huang, Y.; Duan, X. Graphene Nanomesh. *Nat. Nanotechnol.* **2010**, *5*, 190–194.